Is the PTPase−Vanadate Complex a True Transition State Analogue?†

Hua Deng,*,‡ Robert Callender,‡ Zhonghui Huang,§ and Zhong-Yin Zhang§

Departments of Biochemistry and Molecular Pharmacology, Albert Einstein College of Medicine, Bronx, New York 10461

Received December 28, 2001; Revised Manuscript Received March 8, 2002

ABSTRACT: Vanadate can often bind to phosphoryl transfer enzymes to form a trigonal-bipyramidal structure at the active site. The enzyme−vanadate dissociation constants in these enzymes are much lower than those for phosphate. Therefore, enzyme-bound vanadate moieties are often considered as transition state analogues. To test whether the enzyme−vanadate complex is a true transition state analogue beyond the simple geometry and binding affinity arguments and whether the bond orders of the VO bonds in the complex approach those of the PO bonds in the transition state, the binding properties of vanadate in the *Yersinia* protein−tyrosine phosphatase (PTPase) and its T410A, D356N, W354A, R409K, and D356A mutants have been studied by steady-state kinetic measurements and by difference Raman measurements. The results of the kinetic measurements show no correlation between K_I and k_{cat} or k_{cat}/K_m in these mutants. In addition, our analysis of the Raman data shows that the bond order change of the nonbridging V···O bonds in the vanadate complexes does not correlate with the kinetic parameters in a number of PTPase variants as predicted by the transition state binding paradigm. Furthermore, the ionization state of the bound vanadate moiety is not invariant across the PTPase variants studied, and the average bond order of the nonbridging V···O bonds decreased by 0.06−0.07 valence unit in the wild type and all of the mutant PTPases, either in dianionic or in monoanionic form. Thus the complex would resemble an associative transition state, contrary to the previously determined dissociative structure of the transition state. Therefore, it is concluded that vanadate is not a true transition state analogue for the PTPase reactions.

Protein−tyrosine phosphatases (PTPases)[1] have an essential role in signal transduction and, together with protein−tyrosine kinases, control the tyrosine phosphorylation level of proteins in the cell. The *Yersinia* PTPase is one member of this enzyme family. Because of its high enzymatic activity, the *Yersinia* PTPase has been extensively studied as a model system for all PTPases (*1*). The PTPases employ a common catalytic strategy in catalyzing a double-displacement mechanism in which the phosphoryl group is first transferred from the substrate to the active site Cys residue (Cys403 in the *Yersinia* PTPase), leading to the formation of a thiophosphoryl enzyme intermediate that is subsequently hydrolyzed by water. The invariant Arg residue (Arg409 in the *Yersinia* PTPase) functions in substrate binding and in transition state stabilization. The initial phosphoryl transfer step (phosphoenzyme formation) is assisted by general acid catalysis by a conserved Asp (Asp356 in the *Yersinia* PTPase) which protonates the leaving group. The hydrolysis of the phosphoenzyme intermediate is facilitated by the same Asp356, acting as a general base in this catalytic step (for a recent review, see ref *1*).

The early transition metal oxoanion vanadate is a widely used inhibitor for various phosphatases. Vanadate could inhibit phosphatases by simply mimicking the tetrahedral geometry of the phosphate ion. However, in many cases, the enzyme−inhibitor dissociation constant (K_I) for vanadate is much lower than that for phosphate. Because vanadate is known to be able to adopt five-coordinate structures readily, such observations have led to the hypothesis that in some cases vanadate may inhibit phosphatases by forming complexes that resemble the trigonal-bipyramidal geometry of the transition state (*2*, *3*; cf. ref *4*). In the case of PTPases, the binding affinity of vanadate for PTPases is several orders of magnitude higher than that of phosphate (*5*−*8*). To visualize directly the interactions between the PTPase active site and vanadate, the X-ray crystal structure of the *Yersinia* PTPase complexed with vanadate has been determined (*9*). The vanadate moiety in the *Yersinia* PTPase complex is trigonal bipyramidal, with three short equatorial nonbridging V···O bonds, one apical bridging V−O bond, and one long V−S bond to Cys403.[2] Two of the equatorial V···O bonds are hydrogen bounded with two of the Arg409 side chain N−Hs as well as structural water molecules, and the remaining V···O bond is hydrogen bonded to both Val407 and Gly408 backbone N−Hs. The conserved Asp356 makes a hydrogen bond with the apical oxygen of vanadate, consistent with its role as a general acid in the phospho-

† This work was supported in part by Grants GM35183 (R.C.) and CA69202 (Z.-Y.Z.) from the National Institutes of Health.

* Address correspondence to this author: 718-430-2437 (phone); 718-430-8565 (fax); hdeng@medusa.bioc.aecom.yu.edu (e-mail).

‡ Department of Biochemistry.

§ Department of Molecular Pharmacology.

[1] Abbreviations: PTPase, protein−tyrosine phosphatase; *p*NPP, *p*-nitrophenyl phosphate; PTP1B, protein−tyrosine phosphatase 1B.

[2] The nonbridging V···O bonds in a trigonal-bipyramidal structure refer to the bond with unprotonated oxygens, which are always on the equatorial position. In the dianionic form, all three equatorial VO bonds are nonbridging. In the monoanionic form, one of the equatorial oxygens is protonated, and the VO bond becomes a bridging V−O bond. The apical bonds are always bridging bonds since the oxygen is covalently bound to two atoms, one with V and the other with H or other atoms.

10.1021/bi016097z CCC: $22.00
Published on Web 04/06/2002

enzyme formation step and as a general base in the phosphoenzyme hydrolysis step. Similar results have been obtained from structures of vanadate complexes with PTP1B (*10*) and the low molecular weight PTPase (*11*). Collectively, these studies show that vanadate in the PTPase active site adopts a trigonal-bipyramidal geometry that may resemble the transition state for the hydrolysis of the phosphoenzyme intermediate in the PTPase-catalyzed reaction. These studies also support the hypothesis that vanadate inhibits PTPases by acting as a transition state analogue.

The transition state binding paradigm requires that the affinity of an enzyme for a perfect transition state analogue exceed its affinity for the substrate by a factor equivalent to the increased catalytic rate in the enzymatic reaction relative to the corresponding nonenzymatic reaction (*4*). This latter factor has been estimated to be $\sim 10^{10}$- to 10^{11}-fold for the *Yersinia* PTPase, based on the hydrolysis of *p*-nitrophenyl phosphate (*12*). The apparent dissociation constant (K_I) for the *Yersinia* PTPase−vanadate complex is almost 4 orders of magnitude smaller than that of the PTPase−phosphate complex at pH 7.5 (*11*). However, vanadate exists mostly as tetramers and dimers in aqueous solution near neutral pH (*13*). Thus, the affinity of a PTPase for the monomeric vanadate adduct relative to the phosphate is likely more than 2 orders of magnitude larger than that indicated by the apparent K_I values, i.e., at least 10^6-fold stronger than phosphate because of extensive tetra- and dimerization in solution (*14*, *15*). Thus, the PTPase−vanadate complex is likely a plausible transition state mimic, based on both its crystal structure and a simple transition state binding paradigm argument.

One goal of this study is to characterize the interaction between vanadate and PTPase quantitatively at the atomic scale. Raman difference spectroscopy (*16*) is well suited for the determination of high-resolution V···O bond lengths and bond orders of vanadate complexes in enzymes (*17*−*20*), and the measurements report on solution protein complexes. In such studies, the Raman spectrum of the protein−vanadate complex is measured as is that of the protein alone. The difference spectrum between these two spectra contains bands arising from the vanadate group. The vanadate bands dominate the difference spectrum due to their intrinsic large intensity and because most of the protein background spectrum subtracts out (*17*−*19*). The bond lengths and bond orders of the nonbridging V···O bonds as well as the bridging V−O bonds are determined from empirical correlations relating the vibrational stretch frequencies to these quantities (*20*, *21*) The absolute accuracy is very high. The error in these relationships is estimated to be within ±0.04 vu and ±0.004 Å for bond orders and bond lengths, respectively. Moreover, the geometry of the nonbridging V···O bonds, as well as the ionic states of the bound vanadate moiety, can also be ascertained from the vibrational frequencies.

The other goal is to find out if the PTPase−vanadate complex can be treated as a true transition state analogue beyond its geometry and the simple binding paradigm arguments and whether the bond orders of the VO bonds in the complex approach those of the PO bonds in the transition state. First, we argue that if PTPase−vanadate is a true transition state analogue, a simple linear correlation should exist between the binding affinities of vanadate (K_I) and catalytic efficiencies (k_{cat} and/or k_{cat}/K_m) for a series of *Yersinia* PTPase mutants with varying degrees of activity. For a perfect transition state analogue, the correlation will have a slope of unity (*22*, *23*).

In addition, if PTPase−vanadate is a true transition state analogue, changes of the VO bonds in the complex relative to that in solution should be similar to the changes of the PO bonds in the transition state of the PTPase-catalyzed reaction. In general, a phosphoryl transfer reaction can be loosely characterized by three closely related mechanisms: dissociative, S_N2-like, and associative. In a dissociative reaction, the bridging P−O bond breaking of the phosphate compound occurs well before the formation of the new P−O bridging bond in the transition state, the bond order sum of the two apical bridging bonds decreases significantly, and the total bond order sum of the equatorial nonbridging P···O bonds increases significantly compared to the ground state. In a reaction with an S_N2-like transition state, the bond making and bond breaking of the apical P−O bridging bonds in the process are approximately synchronous, and the bond order sum of the corresponding nonbridging P···O bonds is not affected much relative to the ground state. In an associative transition state, the formation of a new P−O bridging bond is well advanced before the breaking of the existing P−O bond, the bond order sum of the two bridging P−O bonds is greatly increased at the transition state, and the bond order sum of the nonbridging P···O bonds is greatly decreased. Results from kinetic isotope measurements of the PTPase-catalyzed reaction as well as observations from linear free energy analysis on the catalyzed rates indicate a dissociative transition state mechanism for the *Yersinia* PTPase (*24*, *25*). Furthermore, the nature of the transition state in many of the mutants under study does not change (*24*−*27*).

Thus, we argue that if the PTPase−vanadate complex is a true transition state analogue, it should be similar to a certain structure of the PTPase−substrate complex along the reaction coordinate toward the transition state. This specific structure can be obtained from the kinetic parameters and the vanadate binding constant based on the quantitative application of the transition state theory. Since all PTPase variants have the same transition state as mentioned above, we can determine this specific structure for each of the PTPase variants, and it should be correlated to the bond order change of the nonbridging V···O bonds upon vanadate binding to PTPase. This method to determine if vanadate complex is a transition state analogue or not is applicable for all reaction mechanisms unless the reaction is strictly S_N2-like.

MATERIALS AND METHODS

A 0.25 M NaH_2VO_4 stock solution was prepared by stirring V_2O_5 with 2 equiv of aqueous NaOH overnight at room temperature. *p*-Nitrophenyl phosphate (*p*NPP) was purchased from Fluka. The catalytic domains of the wild-type *Yersinia* PTPase (residues 163−468) and its mutants D356A, D356N, W354A, R409K, and T410A were expressed under the control of the T7 promoter in *Escherichia coli* BL21(DE3) and grown at room temperature after induction with 0.4 mM IPTG. All recombinant proteins were purified to greater than 95% purity as described previously (*5*, *12*, *24*, *28*−*30*). The catalytic domain of the *Yersinia*

PTPase retains the same activity as the full-length enzyme (*28*) and is used in all of the structural studies (*9*, *31*−*33*). All enzyme assays were performed at 30 °C in either 50 mM Tris at pH 7.5 or 100 mM acetate at pH 5.5 buffers containing 200 mM KCl and 5 mM DTT. Initial rate measurements for the PTPase-catalyzed hydrolysis of pNPP were conducted as previously described (*28*). The Michaelis−Menten kinetic parameters were determined from a direct fit of the *V* vs [S] data to the Michaelis−Menten equation using the nonlinear regression program GraFit (Erithacus Software). The range of *p*NPP concentration used was from 0.2 to 5 K_m. In all cases, the enzyme concentration was much lower than that of the substrate so that the steady-state assumption was fulfilled. Inhibition constants (K_I) for the PTPase by vanadate were determined with *p*NPP as substrate. The mode of inhibition and the K_I value were determined in the following manner. At various fixed concentrations of inhibitor (0−3 K_I), the initial rate at a series of *p*NPP concentrations was measured ranging from 0.2 to 5 of the apparent K_m values. The data were fitted to appropriate equations using kinetAsyst to obtain the inhibition constant and to assess the mode of inhibition.

The enzyme samples for spectroscopic measurements were prepared by extensive dialysis in 50 mM Tris at pH 7.5 or 100 mM acetate at pH 5.5, respectively, with 200 mM KCl and 5 mM DTT, followed by concentration with a Centricon 30 centrifuge concentrator (Amicon, Lexington, MA) to the desired concentration. The concentrations of the PTPase were determined spectroscopically using a molar extinction coefficient of 16800 M^{-1} cm^{-1} at 280 nm for the catalytic domain of the *Yersinia* PTPase. The binary complex of the PTPase−vanadate complex was prepared by adding the vanadate stock solution to the concentrated PTPase sample to achieve a molar ratio of 0.9:1. The typical concentration of the PTPase sample was about 5 mM.

The Raman spectra were measured using an optical multichannel analyzer (OMA) system. The OMA system uses a Triplemate spectrometer (Spex Industries, Metuchen, NJ) with a model DIDA-1000 reticon detector connected to an ST-100 detector (Princeton Instruments, Trenton, NJ). Details of the system can be found elsewhere (*16*). The 514.5 nm line from an argon ion laser (model 165, Spectra Physics, Mountain View, CA) was used to irradiate the sample (∼100 mW). A half-wave retarder was used to polarize the incident light either parallel or perpendicular to the entrance slit of the spectrometer. The symmetry of a vibrational mode was assessed in terms of the ratio of Raman intensities obtained with the excitation beam in the perpendicular and parallel configurations. In this optical arrangement, the intensity ratios are 6:7 for an asymmetric mode and <6:7 for a symmetric mode for the optical configuration used here (*34*). (This geometry, rather than the more common geometry that determines the "depolarization ratio", was employed to maximize signal throughput.) The polarization response of the spectrometer was calibrated by measurements of the toluene spectrum, where the symmetry of the various bands is known.

Separate spectra for enzyme and enzyme−vanadate complexes in solution, approximate concentration of 5 mM, were measured using a special split cell (the volume of each side being about 30 μL) and a sample holder with a linear translator as previously described (*16*). The spectrum from one side of the split cuvette is taken, the split cell is translated, and the spectrum from the other side is taken. This sequence is repeated until sufficient signal to noise is obtained. A difference spectrum is generated by numerically subtracting the sum of the spectra obtained from each side. In general, the two summed spectra do not subtract to zero, as judged by the subtraction of well-known protein marker bands (for example, the amide I, amide III, and the phenylalanine 1004 cm^{-1} bands, the latter band being especially useful since it is generally not affected by protein conformational changes). These protein marker bands are determined from their bandwidths (generally much broader than those from spectra of bound substrates) and their characteristic positions. Hence, one summed spectrum is scaled by a small numerical factor, generally between 1.05 and 0.95, which is adjusted until the protein bands are nulled (see, e.g., ref *35*). The same control procedures were performed on all the difference spectra results herein. Resolution of the spectrometer is 8 cm^{-1} for the present results. A spectral calibration is done for each measurement using the known Raman lines of toluene, and absolute band positions are accurate to within ±2 cm^{-1}. None of the spectra presented here have been smoothed.

RESULTS

On the basis of the transition state theory, if the PTPase−vanadate complex is a perfect transition state analogue, then one would expect to observe a linear correlation with a slope of unity between the binding affinity of PTPase variants for vanadate (K_I) and the catalytic efficiency of the PTPase variants (k_{cat} or k_{cat}/K_m). The slope would be less than unity for the not so perfect transition state analogue (*22*, *23*). To determine if such a correlation exists, we have prepared the wild-type *Yersinia* PTPase and the D356A, D356N, Arg409, W354A, and T410A mutants. The roles of these residues in catalysis are well characterized, and the mutant PTPases display a wide range of activity. Extensive mechanistic studies suggest that Asp356 is the general acid/base (*12*, *25*) that interacts with the apical oxygen of vanadate, which most closely resembles the leaving group oxygen or the attacking water in the transition state (*9*). The side chain of the invariant Arg409 forms a bidentate hydrogen bond with two of the nonbridging phosphoryl oxygens (*33*), and kinetic analyses of the Arg409 mutants indicate that Arg409 plays an important role in both substrate binding and transition state stabilization (*24*, *26*). Trp354 is important for the correct positioning of Arg409 and Asp356 in a catalytically competent conformation (*31*, *36*). Interestingly, mutations of Trp354 lead to the impairment of both Arg409 and Asp356 (*27*, *36*). The hydroxyl group of Thr410 immediately following the invariant Arg409 functions to stabilize the thiolate anion during the breakdown of the phosphoenzyme intermediate (*37*−*39*).

Kinetic parameters of the wild-type *Yersinia* PTPase and its T410A, D356N, W354A, R409K, and D356A mutants were obtained according to the procedure described in Materials and Methods. The k_{cat} and K_m for the enzyme-catalyzed hydrolysis of pNPP and the K_I values for vanadate at pH 7.5 are listed in Table 1. Among these mutant PTPases, the k_{cat} and k_{cat}/K_m values vary by almost 4 orders of magnitude. The K_I values vary from 0.24 μM in T410A to 204 μM in R409K, a difference of 3 orders of magnitude.

Table 1: Steady-State Kinetic Parameters for the PTPase-Catalyzed Hydrolysis of *p*-Nitrophenol Phosphate and Inhibition Constant of Vanadate at pH 7.5 and 5.5[a]

	pH 7.5						pH 5.5		
	WT	T410A	D356N	W354A	R409K	D356A	WT	T410A	D356N
k_{cat} (s^{-1})	17	11.8	0.418	0.269	0.0113	0.00293	651	17.2	0.417
K_m (mM)	3.03	3.83	2.63	4.57	7.4	0.289	4.95	0.14	3.74
k_{cat}/K_m (s^{-1} mM^{-1})	5.61	3.08	0.159	0.059	0.00153	0.0101	132	123	0.111
K_I (μM)	1.23	0.24	2.06	11	204	0.442	1.12	0.223	0.479
σ	0.34	0.43	0.375	0.32	0.23	0.46	0.32	0.28	0.47

[a] The measurements were performed at either pH 7.5 in 50 mM Tris buffer or pH 5.5 in 100 mM acetate buffer containing 0.2 M KCl and 1 mM DTT at 303 K. σ is the ratio of $\log(K_m/K_I)$ and $\log[k_{cat}/k_{cat}(\text{solution})]$.

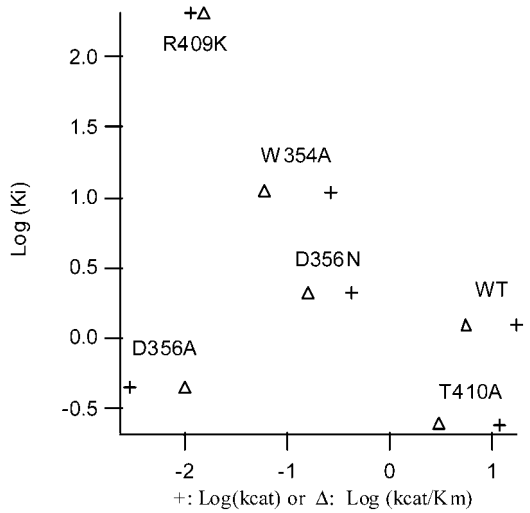

FIGURE 1: Plots of log K_I of vanadate versus log k_{cat} (+) and log k_{cat}/K_m (△) in PTPase and its mutants.

In all cases, the competitive inhibition pattern was observed for vanadate, suggesting that vanadate binds to the active site of PTPase and its mutants regardless of its ionic state.

Previous studies have shown that the kinetic parameter k_{cat}/K_m monitors the phosphoenzyme formation step whereas k_{cat} follows the hydrolysis of the phosphoenzyme intermediate (*12*, *25*, *30*, *37*, *38*, *40*). Figure 1 shows the plot of K_I versus either k_{cat} or k_{cat}/K_m in log scale. There is no apparent correlation between K_I and k_{cat} or k_{cat}/K_m when all data points are considered. Such results would suggest that PTPase−vanadate is not a transition state analogue for either the enzyme phosphorylation step or the step of hydrolysis of the phosphorylated enzyme. If one can omit the data point for D356A and consider only the wild type and D356N, W354A, T410A, and R409 mutants, a reasonably good correlation between log K_I and log k_{cat}/K_m or log k_{cat} with a slope quite close to unity is found. However, we do not have compelling evidence to exclude D356A in the analysis because although D356A is a less conservative change than D356N, the transition state properties are the same for both mutants (*25*, *26*, *41*).

We next performed Raman difference spectroscopy experiments in order to study the interaction between vanadate and the PTPases quantitatively at the atomic scale. The measurements of the nonbridging V⋯O stretch mode frequencies of the vanadate bound in *Yersinia* PTPase and one of its mutants, D356A, as well as those of the vanadate solution model compounds are presented in Figure 2. Since the PTPase−vanadate complex has a thiol ligand, a better solution model compound would be mono- and dianionic thiovanadate. Unfortunately, several attempts to form a stable mono- and dianionic thiovanadate in solution were unsuccessful. Since the apical V−S bond is normally weaker than apical V−O bond, the nonbridging V⋯O bond would be stronger and their stretch frequencies should be higher in thiovanadate than in oxovanadate. Frequency calculations based on ab initio methods suggest that the nonbridging V⋯O stretch frequency in a thiovanadate should be about 20 cm^{-1} higher than its oxo counterpart in the monoanionic form and quite comparable in the dianionic form. The solution structures of various vanadate compounds have been studied by a number of methods, including Raman. It turned out that the frequency of the nonbridging V⋯O stretch modes of solution vanadate depends primarily on its ionic state, being 870 ± 5 cm^{-1} for dianionic vanadate and ∼940 ± 10 cm^{-1} for monoanionic vanadate, and the nonbridging V⋯O stretch frequency in a $V-O-VO_2$ structure is about 10−15 cm^{-1} higher compared to that in a $C-O-VO_2$ structure (*14*, *15*, *17*, *18*). Thus, the vanadate tetramers in aqueous solution are chosen to model the PTPase−vanadate complex to partially compensate for the expected V⋯O stretch frequency change due to the thio effect. The error introduced here would just add a small offset to the bond order change and would not affect our subsequent analysis.

In each of the four panels in Figure 2, two Raman spectra are shown. The spectrum using the parallel polarized incident laser beam is plotted on the top and the spectrum obtained with the perpendicular polarized laser beam is on the bottom. In all cases, the most dominant band in the parallel polarized spectrum is the symmetric V⋯O stretch mode, and the intensity of this mode decreased in the perpendicular polarized spectrum so that the asymmetric V⋯O stretch mode becomes the major band(s). Panel a in Figure 2 shows the Raman spectra of vanadate in solution at pH 7.5. At this pH, vanadate is monoanionic and therefore contains two nonbridging V⋯O bonds. The stretch motions of the two nonbridging bonds are strongly coupled to form a symmetric V⋯O stretch mode and an asymmetric V⋯O stretch. The intensity of the vibrational modes from bridging V−O stretches is too weak to be observed in the Raman spectra. The band at 945 cm^{-1} in the top spectrum is the symmetric V⋯O stretch mode, and the band at 922 cm^{-1} in the bottom spectrum is the asymmetric stretch mode. Panel b in Figure 2 shows the Raman spectra of vanadate in solution at pH 10. At this pH, vanadate is dianionic and therefore contains three nonbridging V⋯O bonds. The band at 870 cm^{-1} and the band at 869 cm^{-1} are assigned to symmetric V⋯O stretch and the doubly degenerated asymmetric V⋯O stretch mode,

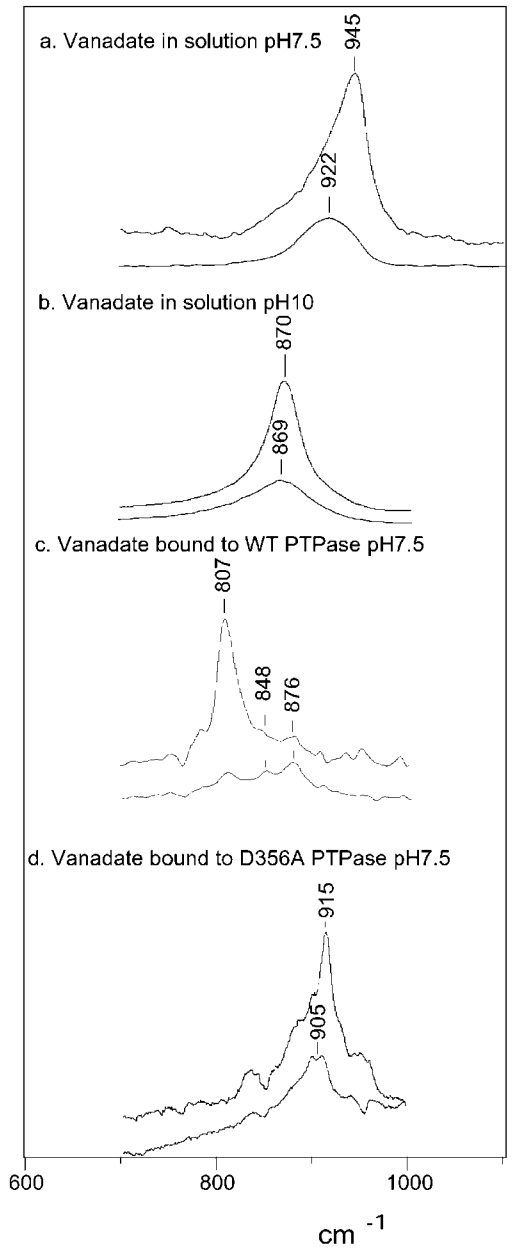

FIGURE 2: (a) Raman spectra of 100 mM NaH_2VO_4 at pH 7.5. (b) Raman spectra of 100 mM Na_2HVO_4 at pH 10. (c) Raman difference spectra of the WT PTPase−vanadate complex minus PTPase at pH 7.5 at 4 °C. (d) Raman difference spectra of the D356A−vanadate complex minus D356A at pH 7.5 at 4 °C. In all panels, two spectra are presented. One was obtained with a parallel polarized excitation beam (top) and one with a perpendicular polarized beam (bottom). Only nonbridging V⋯O stretch modes are observed in the presented spectral range. The enzyme samples are prepared in 50 mM Tris at pH 7.5 with 300 mM NaCl and 5 mM DTT. The concentration of PTPase/vanadate in the complex was about 5 mM/4.5 mM. The 514.5 nm line from an argon ion laser was used to irradiate the sample (∼100 mW). The spectral resolution was 8 cm^{-1}.

respectively. These two modes happen to have the same frequency.

Panel c in Figure 2 shows the Raman difference spectra between the wild-type PTPase−vanadate complex and wild-type PTPase at pH 7.5. The band at 807 cm^{-1} is assigned to the symmetric V⋯O stretch mode, and the minor band in the parallel polarized spectrum at 876 cm^{-1} is assigned to the asymmetric V⋯O stretch mode. The presence of a third band at 848 cm^{-1}, which has an intensity ratio intermediate between a symmetric (perpendicular to parallel polarized intensity ratio near zero) and an asymmetric mode (ratio of 6:7), suggests that the C_{3v} symmetry of the vanadate dianion in solution has been broken when vanadate binds to the wild-type PTPase. That the symmetry of the three V⋯O bonds in the complex is somewhat altered from a nearly perfect C_{3v} symmetry in solution is also consistent from the observation that the intensity ratio of the "symmetric" V⋯O stretch mode in the complex at 807 cm^{-1} using perpendicular polarized laser light compared to parallel polarized light is significantly larger than zero, as shown by the finite intensity of the band at 807 cm^{-1} in the perpendicular polarized spectrum (panel c, Figure 2). The assignments of these bands are also supported by vibrational analysis using ^{18}O labeling of the vanadate and ab initio calculations (*19*). A comparison with the vanadate solution spectra (panels a and b) shows that the vanadate bound in the wild-type PTPase is dianionic at pH 7.5. The relatively large difference between the Raman frequencies of the vanadate nonbridging V⋯O bond stretch modes in wild-type PTPase (panel c, Figure 2) and the dianionic vanadate in solution (panel b, Figure 2) indicates a significant bond order decrease of the nonbridging V⋯O bonds in the PTPase complex and geometry change (see below).

Similar measurements were also performed on several mutant forms of the PTPase, including D356N, D356A, W354A, R409K, and T410A. The observed nonbridging V⋯O stretch frequencies of the vanadate moiety in these mutant complexes are listed in Table 2. The spectra of D356N and T410A are similar to that of wild-type PTPase while the spectra of D356A, R409K, and W354A are similar to each other but very different from that of wild type.

Panel d in Figure 2 shows the Raman difference spectra between D356A mutant PTPase/vanadate and D356A PTPase at pH 7.5. The band at 905 and 915 cm^{-1} in these two spectra can be assigned to asymmetric and symmetric V⋯O stretch modes, respectively. The question that remains is whether the vanadate moiety in this complex is monoanionic or dianionic. Additional Raman measurements show that there is no significant change of the V⋯O stretch modes in the wild-type and D356A mutant vanadate complex when the sample pH is decreased to 5.5. However, in the D356N−vanadate complex, about 80% of the symmetric V⋯O stretch mode intensity shifts up from 807 cm^{-1} at pH 7.5 to 911 cm^{-1} at pH 5.5, clearly indicating a titration of vanadate from dianionic to monoanionic form (data not shown). Since the V⋯O stretch band positions in the D356A and D356N mutants are the same at pH 5.5, we conclude that the vanadate moiety in the D356A complex is monoanionic at pH 7.5. Furthermore, since vanadate still demonstrates a competitive inhibition property in the steady-state kinetic measurements at pH 5.5, the binding site for vanadate at pH 5.5 and at pH 7.5 should be the same active site. Thus, our results ruled out the possibility of an increased bond order of the nonbridging V⋯O bonds in the D356A−vanadate complex compared to its solution model compound. The symmetric stretch frequency of vanadate nonbridging V⋯O bonds in PTPase shifts down by 30 cm^{-1} from its solution value while the asymmetric mode frequency shifts down by 17 cm^{-1} (compare panels a and d in Figure 2), indicating a significant nonbridging V⋯O bond order decrease when vanadate binds in these mutants as a monoanion.

Table 2: Bond Order and Bond Length Changes of the Nonbridging V⋯O Bond Calculated from the V⋯O Stretch Frequencies of Vanadate upon Binding to PTPase and Its Mutants[a]

	$-VO_3^{2-}$	WT	T410A	D356N	$>VO_2^-$	W354A	R409K	D356A
ν_s	870	807	805	806	945	915	920	915
ν_{as1}	869	848	845	845	922	905	890	905
ν_{as2}	869	876	880	880				
ν	869	844	844	844	934	910	905	910
S_{VO} (vu)	1.431	1.366	1.365	1.366	1.605	1.540	1.527	1.540
ΔS_{VO}		−0.065	−0.066	−0.065		−0.065	−0.079	−0.065
R_{VO} (A)	1.669	1.685	1.685	1.685	1.632	1.646	1.648	1.646
ΔR_{VO}		0.015	0.015	0.015		0.013	0.016	0.013

[a] ν_s is the symmetric nonbridging V⋯O stretch mode and $\nu_{as1(2)}$ is the asymmetric nonbridging V⋯O stretch mode. ν is the fundamental frequency, equal to the square root of average frequency squares of all ν_s and ν_{as} frequencies (*20*). S_{VO} is the average bond order of the nonbridging V⋯O bonds calculated from ν using eqs 1 and 2. ΔS_{VO} is bond order difference relative to dianionic vanadate, $-VO_3^{2-}$, for WT, T410*A* and D356N and relative to monoanionic vanadate, $>VO_2^-$, for W354A, R409K, and D356A. R_{VO} is the average bond order of the nonbridging V⋯O bonds calculated from ν using eqs 1 and 2. ΔR_{VO} is the bond order difference relative to dianionic vanadate, $-VO_3^{2-}$, for WT, T410A, and D356N and relative to monoanionic vanadate, $>VO_2^-$, for W354A, R409K, and D356A.

Accurate structural information about bonding in vanadate can be obtained from vibrational spectroscopy by using two types of empirical relationships. One is the bond length/bond strength correlation (*42*, *43*); the other is the bond strength/vibrational frequency correlation (*20*).

These two correlations are given by the equations (*20*)

$$S_{VO} = (R_{VO}/1.791)^{-5.1} \quad (1)$$

and

$$S_{VO} = [0.2912 \ln(21349/\nu)]^{-5.1} \quad (2)$$

where S_{VO} and R_{VO} are the bond order and bond length of a VO bond, respectively, and ν is the nonbridging V⋯O stretching frequency. The appropriate frequency to be used in eq 2 is the geometric mean of the observed nonbridging V⋯O stretches; $\nu = [(\nu_s^2 + 2\nu_a^2)/3]^{1/2}$ (ν_s is the symmetric stretch and ν_a the asymmetric stretch) when the VO_3 moiety retains nominal $C_{3\nu}$ symmetry, or, when the symmetry of the VO_3^{2-} moiety is somewhat broken, like the vanadate in wild-type PTPase, $[(\nu_1^2 + \nu_2^2 + \nu_3^2)/3]^{1/2}$ to determine the average bond order and bond length of the three nonbridging V⋯O bonds. The absolute error in these relationships in determining bond lengths and bond orders from frequency measurements is estimated to be within ±0.04 vu and ±0.004 Å for bond orders and bond lengths, respectively (*20*), and more accurate for determining bond length and bond order changes.

The "fundamental" frequency of the dianionic vanadate solution model is calculated to be 869.3 cm^{-1} from ν_s = 870 cm^{-1} and ν_a = 869 cm^{-1}, which yields a bond order of 1.430 vu and a bond length of 1.669 Å for each of the three nonbridging V⋯O bonds using eqs 1 and 2. The shift to lower frequency for the V⋯O bonds in the wild-type PTPase-bound vanadate translates to a somewhat lower bond order and longer bond length for the three bonds. From eqs 1 and 2, the three frequencies at 807, 848, and 876 cm^{-1} yield an average frequency of 848 cm^{-1} and an average bond order and bond length of 1.366 vu and 1.685 Å, respectively. Compared with the solution values, they change by −0.065 vu and +0.015 Å, respectively (Table 2).

The fundamental frequency of the monoanionic vanadate solution model is calculated to be 933.5 cm^{-1} from ν_s = 945 cm^{-1} and ν_a = 922 cm^{-1}, which yields a bond order of 1.605 vu and a bond length of 1.632 Å for each of the two nonbridging V⋯O bonds using eqs 1 and 2. The shift to lower frequency for the V⋯O bonds in the D356A PTPase-bound vanadate translates to a somewhat lower bond order and longer bond length for the three bonds. From eqs 1 and 2, the two frequencies at 905 and 915 cm^{-1} yield an average frequency of 910 cm^{-1} and an average bond order and bond length of 1.540 vu and 1.646 Å, respectively. Compared with the solution values, these parameters change by −0.065 vu and +0.013 Å, respectively, upon binding. It is interesting to note that when the active site Arg409 is mutated to Lys, the polarization of the nonbridging V⋯O bonds is actually increased somewhat compared with other PTPase variants (see Table 2).

DISCUSSION

Previous studies on RNase suggested that the RNase−uridine−vanadate complex may indeed be a true transition state analogue. The Raman studies of this complex suggested that there is a loss of 0.11−0.22 valence unit of the nonbridging P⋯O bonds in the transition state, based on the bond order change of the nonbridging V⋯O bonds in the complex (*15*). Studies on the secondary ^{18}O isotope effects in the RNase-catalyzed reaction suggested that the total bond order of the nonbridging P⋯O bonds loses 0.13−0.20 valence unit in the transition state (*44*). However, such quantitative agreement can be interpreted as a coincidence because of limited available data.

To avoid any coincidence, a number of carefully chosen PTPase variants with a wide range of catalytic efficiencies have been used in the steady-state kinetic measurements to determine if a linear correlation between the binding affinity for vanadate (K_I) and the k_{cat} or k_{cat}/K_m exists. Such correlation is expected on the basis of the transition state binding paradigm. As a whole, our data show no indication of linear correlation (Figure 1). However, when the data point from D356A is excluded from the figure, a reasonable linear correlation is observed. Since the transition state properties are the same for both D356A and D356N (*25*, *26*, *41*), there is no obvious reason to exclude this point. Thus, our results suggest that PTPase−vanadate is unlikely a true transition state analogue beyond the geometry similarity.

Our Raman studies on the PTPase−vanadate complexes also support this conclusion. On the basis of the transition state binding paradigm, we argue that if vanadate moiety in this enzyme is a true transition state analogue, the nonbridg-

ing V···O bond order change upon vanadate binding to this series of PTPase variants should reflect the P···O bond order change of the substrate in a specific structure along the reaction coordinate toward the transition state. Where this structure is located along the reaction path in the free energy diagram can be determined by using the kinetic parameters and vanadate binding constant. For a perfect transition state analogue, the logarithm of the ratio of [1/*K*(vanadate)]/[1/*K*(substrate)] should be equal to the logarithm of the rate enhancement in the PTPase-catalyzed reaction. For a non-perfect transition state analogue, the ratio of these two values will indicate where the analogue is along the reaction pathway. This ratio was calculated for each PTPase variant and is listed in Table 1. According to this value, for wild-type PTPase, the vanadate complex would be an analogue of a state 34% on the way along the reaction path toward the transition state at pH 7.5, if it is a transition state analogue. For other PTPase variants under various conditions, the vanadate complexes would be from 23% to 45% of the way. Since previous studies have shown that the nature of the transition state in all PTPase variants is the same (*24*−*27*), we expect that the nonbridging V···O bond order changes in these vanadate complexes would be correlated with these numbers. However, it is clear from Table 1 that no such correlation exists since the nonbridging V···O bond order changes are the same for all PTPase variants. In addition, if the PTPase−vanadate complex were a true transition state analogue in the sense that the nonbridging V···O bonds in the complex undergo changes similar to that of the nonbridging P···O bonds in the transition state of the PTPase-catalyzed reaction, our results would indicate an S_N2-like transition state, with a small associative character. Such prediction is not consistent with the results from previous studies of several types of PTPases on both phosphorylation and dephosphorylation steps, indicating a dissociative transition state (*12*, *24*−*27*, *30*, *38*, *41*). In this case, the apical bonds of the bound pentacoordinated VO_3^{2-} fragment are close to zero should vanadate bind to PTPase with a structure close to that of the transition state. Hence, it is expected that the sum of the apical bonds of bound vanadate is substantially lower than the HO−VO_3^{2-} bond of vanadate in solution. According to the valance bond paradigm used in the analysis here for relating bond orders (and lengths) to vibrational frequencies, the sum of the bond order about the metal atom remains constant (equal to 5 for vanadium). Hence, the finding that the total bond order of the nonbridging V···O bonds *decreases* by 0.195 vu (three times 0.065) for the wild-type protein (Table 2) when vanadate binds to the protein means that the sum of the bond order in the apical bonds *increases* by the same amount, completely contrary to the putative dissociative transition state structure. It is also contrary to the idea of a transition state mimic for its ionization state to change for the wild-type proteins and mutants assuming, reasonably, that the structure of the transition state remains the same for the various proteins (i.e., dissociative, S_N2, or associative-like). Hence, the finding that the bound vanadate moiety is dianionic for wild-type PTPase and the T410A and D356N mutants, while monoanionic for the W354A, R409K, and D356A proteins, strongly argues against the idea of vanadate as a true transition state analogue.

Although our results show that PTPase−vanadate is not a true transition state analogue, interesting information about the interactions between vanadate and PTPase has been derived from our studies of this complex. For example, the ionic state of the bound vanadate in various mutants is determined. In the wild-type PTPase, the pK_a of the −VO_3^{2-} group is apparently reduced by at least 3 pH units, from about pH 8.5 in solution to below pH 5.5. This is also true for T410A. In some of the mutants such as D356A, R409K, and W354A, the pK_a of bound vanadate does not change from the solution value so that the bound vanadate in those mutants near neutral pH remains monoanionic. In D356N, the pK_a of the bound vanadate is decreased by about 2 pH units compared to the vanadate in solution. The bond order and bond length of the nonbridging V···O bonds in the complex can be determined quantitatively from their Raman measurements. Since the V···O bond order is a direct reflection of the hydrogen-bonding strength on the V···O bond, we can also conclude that the hydrogen-bonding strength on the nonbridging V···O bonds of the vanadate moiety is not affected by D356N and T410A mutations at pH 7.5, and the hydrogen-bonding strength on the remaining two nonbridging V···O bonds does not change much when the vanadate moiety is changed from dianionic to monoanionic in D356N. Furthermore, since the K_I values range from 0.24 μM in T410A to 1.23 μM in wild-type PTPase for dianionic vanadate and from 0.44 μM to 204 μM in monoanionic form, and since the interactions of the nonbridging V···O bonds do not vary much among wild-type and mutant PTPases, the large difference in the binding affinity of vanadate must be due to the differences of the V−S bond and the interaction of V−OH bridging bonds with the enzyme.

Our Raman studies also show that the active site of the PTPase is capable of polarizing the nonbridging V···O bonds, no matter whether the vanadate moiety is dianionic or monoanionic. The X-ray crystallographic studies show that the polarization of the nonbridging V···O bonds is apparently facilitated by the backbone N−H groups, the side chain NHs of Arg409, and active site water molecules. It is often observed that the same type of hydrogen bonding is stronger in the hydrophobic environment than in the hydrophilic environment (*45*, *46*). This and other observations had lead to the proposal that the coordination of the active site positively charged residues with nonbridging P···O bonds of the phosphate compounds could be stronger than that in aqueous solution in phosphoryl transfer enzyme, so that a transition state with more associative character would be favored in the enzyme compared to the solution reaction (for a brief discussion and references, see ref *47*). Our results show quantitatively that the enzyme active site is capable of rendering stronger hydrogen bonding to the nonbridging P···O bonds as indicated by the 0.066 vu bond order decrease of the V···O bonds in the PTPase−vanadate complex. However, this is not happening in the transition state since it has been well established that the PTPase-catalyzed phosphoryl transfer reaction is dissociative; thus the coordination to the nonbridging P···O bonds is weakened in the transition state. Apparently, further studies are in order to solve this puzzle.

REFERENCES

1. Zhang, Z.-Y. (1998) *Crit. Rev. Biochem. Mol. Biol. 33*, 1−52.
2. Lindquist, R. N., Lynn, J. L. J., and Lienhard, G. E. (1973) *J. Am. Chem. Soc. 95*, 8762−8768.

3. VanEtten, R. L., Waymack, P. P., and Rehkop, D. M. (1974) *J. Am. Chem. Soc. 96*, 6782−6785.
4. Gandour, R. D., and Schowen, R. L. (1987) *Transition States of Biochemical Processes*, pp 1−616, Plenum Press, New York.
5. Wu, L., Buist, A., den Hertog, J., and Zhang, Z.-Y. (1997) *J. Biol. Chem. 272*, 6994−7002.
6. Huyer, G., Liu, S., Kelly, J., Moffat, J., Payette, P., Kennedy, B., Tsaprailis, G., Gresser, M. J., and Ramachandran, C. (1997) *J. Biol. Chem. 272*, 843−851.
7. Wang, F., Li, W., Emmett, M. R., Hendrickson, C. L., Marshall, A. G., Zhang, Y.-L., Wu, L., and Zhang, Z.-Y. (1998) *Biochemistry 37*, 15289−15299.
8. Zhou, B., and Zhang, Z.-Y. (1999) *J. Biol. Chem. 274*, 35526−35534.
9. Denu, J. M., Lohse, D. L., Vijayalakshmi, J., Saper, M. A., and Dixon, J. E. (1996) *Proc. Natl. Acad. Sci. U.S.A. 93*, 2493−2498.
10. Pannifer, A. D., Flint, A. J., Tonks, N. K., and Barford, D. (1998) *J. Biol. Chem. 273*, 10454−10462.
11. Zhang, M., Zhou, M., Van Etten, R. L., and Stauffacher, C. (1997) *Biochemistry 36*, 15−23.
12. Zhang, Z.-Y., Wang, Y., and Dixon, J. E. (1994) *Proc. Natl. Acad. Sci. U.S.A. 91*, 1624−1627.
13. Tracey, A. S., Gresser, M. J., and Liu, S. (1988) *J. Am. Chem. Soc. 110*, 5869−5874.
14. Ray, W. J., Crans, D. C., Zheng, J., Burgner, J. W., Deng, H., and Mahroof-Tahir, M. (1995) *J. Am. Chem. Soc. 117*, 6015−6026.
15. Deng, H., Burgner, J., and Callender, R. (1998) *J. Am. Chem. Soc. 120*, 4717−4722.
16. Callender, R., and Deng, H. (1994) *Annu. Rev. Biophys. Biomol. Struct. 23*, 215−245.
17. Ray, J. W. J., Burgner, I. J. W., Deng, H., and Callender, R. (1993) *Biochemistry 32*, 12977−12983.
18. Deng, H., Ray, W. J., Jr., Burgner, J. W., II, and Callender, R. (1993) *Biochemistry 32*, 12984−12992.
19. Deng, H., Wang, J., Callender, R. H., Grammer, J. C., and Yount, R. G. (1998) *Biochemistry 37*, 10972−10979.
20. Deng, H., Wang, J., Ray, W. J., and Callender, R. (1998) *J. Phys. Chem. B 102*, 3617−3623.
21. Hardcastle, F. D., and Wachs, I. E. (1991) *J. Phys. Chem. 95*, 5031−5041.
22. Messmore, J. M., and Raines, R. T. (2000) *J. Am. Chem. Soc. 122*, 9911−9916.
23. Bartlett, P. A., and Marlowe, C. K. (1983) *Biochemistry 22*, 4618−4624.
24. Zhang, Y.-L., Hollfelder, F., Gordon, S. J., Chen, L., Keng, Y.-F., Wu, L., Herschlag, D., and Zhang, Z.-Y. (1999) *Biochemistry 38*, 12111−12123.
25. Hengge, A. C., Sowa, G. A., Wu, L., and Zhang, Z.-Y. (1995) *Biochemistry 34*, 13982−13987.
26. Hoff, R. H., Wu, L., Zhou, B., Zhang, Z.-Y., and Hengge, A. C. (1999) *J. Am. Chem. Soc. 121*, 9514−9521.
27. Hoff, R. H., Hengge, A. C., Wu, L., Keng, Y.-F., and Zhang, Z.-Y. (2000) *Biochemistry 39*, 46−54.
28. Zhang, Z.-Y., Clemends, J. C., Schubert, H. L., Stuckey, J. A., Fisher, M. W. F., Hume, D. M., Saper, M. A., and Dixon, J. E. (1992) *J. Biol. Chem. 267*, 23759−23766.
29. Zhang, Z.-Y., Wang, Y., Wu, L., Fauman, E., Stuckey, E., Schubert, H. L., Saper, M. A., and Dixon, J. E. (1994) *Biochemistry 33*, 15266−15270.
30. Zhang, Z.-Y., Wu, L., and Chen, L. (1995) *Biochemistry 34*, 16088−16096.
31. Schubert, H. L., Fauman, E. B., Stuckey, J. A., Dixon, J. E., and Saper, M. A. (1995) *Protein Sci. 4*, 1904−1913.
32. Fauman, E. B., Yuvaniyama, C., Schubert, H. L., Stuckey, J. A., and Saper, M. A. (1996) *J. Biol. Chem. 271*, 18780−18788.
33. Stuckey, J. A., Schubert, H. L., Fauman, E., Zhang, Z. Y., Dixon, J. E., and Saper, M. A. (1994) *Nature 370*, 571−575.
34. Wilson, E. B. J., Decius, J. C., and Cross, P. C. (1955) *Molecular Vibrations*, McGraw-Hill, New York.
35. Deng, H., Kurz, L., Rudolph, F., and Callender, R. (1998) *Biochemistry 37*, 4968−4976.
36. Keng, Y.-F., Wu, L., and Zhang, Z.-Y. (1999) *Eur. J. Biochem 259*, 809−814.
37. Zhang, Z.-Y., Palfey, B. A., Wu, L., and Zhao, Y. (1995) *Biochemistry 34*, 16389−16396.
38. Zhao, Y., and Zhang, Z.-Y. (1996) *Biochemistry 35*, 11797−11804.
39. Denu, J. M., and Dixon, J. E. (1995) *Proc. Natl. Acad. Sci. U.S.A. 92*, 5910−5914.
40. Zhao, Y., Wu, L., Noh, S. J., Guan, K.-L., and Zhang, Z.-Y. (1998) *J. Biol. Chem. 273*, 5484−5492.
41. Hengge, A. C., Zhao, Y., Wu, L., and Zhang, Z.-Y. (1997) *Biochemistry 36*, 7928−7936.
42. Brown, I. D. (1992) *Acta Crystallogr. B48*, 553−572.
43. Brown, I. D., and Wu, K. K. (1976) *Acta Crystallogr. B32*, 1957−1959.
44. Sowa, G. A., Hengge, A. C., and Cleland, W. W. (1997) *J. Am. Chem. Soc. 119*, 2319−2320.
45. Jeffrey, G. A., and Saenger, W. (1991) *Hydrogen Bonding in Biological Structures*, Springer-Verlag, Berlin.
46. Vinogradov, S. N., and Linnel, R. H. (1971) *Hydrogen Bonding*, Van Nostrand Reinhold Co., New York.
47. O'Brien, P. J., and Herschlag, D. (1999) *J. Am. Chem. Soc. 121*, 11022−11023.

BI016097Z